Optimal Algorithm Switching for the Estimation of Systole Period From Cardiac Microacceleration Signals (SonR)

Lionel Giorgis [1 2], Paul Frogerais [1], Amel Amblard [2], Erwan Donal [1 3], Philippe Mabo [1 3], Lotfi Senhadji [1], Alfredo Hernandez [1 *]

[1] LTSI, Laboratoire Traitement du Signal et de l'Image INSERM : U1099 , Université de Rennes 1 , 263, avenue du Général Leclerc 35042 Rennes Cedex, FR

[2] Sorin CRM Centre d'Excellence - Sorin Group , 4 avenue R??aumur 92140 Clamart, FR

[3] Service de Cardiologie et Maladies Vasculaires Hôpital Pontchaillou , Université de Rennes 1 , CHU Rennes , 2 rue Henri Le Guilloux 35033 Rennes Cedex 9, FR

* Correspondence should be addressed to: Alfredo Hernandez <alfredo.hernandez@univ-rennes1.fr >

Abstract

Previous studies have shown that cardiac micro-acceleration signals, recorded either cutaneously, or embedded into the tip of an endocardial pacing lead, provide meaningful information to characterize the cardiac mechanical function. This information may be useful to personalize and optimize the cardiac resynchronization therapy, delivered by a biventricular pacemaker, for patients suffering from chronic heart failure. The present paper focuses on the improvement of a previously proposed method for the estimation of the systole period from a signal acquired with a cardiac micro-accelerometer (SonR sensor, Sorin CRM SAS, France). We propose an optimal algorithm switching approach, to dynamically select the best configuration of the estimation method, as a function of different control variables, such as signal-to-noise ratio or heart rate. This method was evaluated on a database containing recordings from 31 patients suffering from chronic heart failure and implanted with a biventricular pacemaker, for which various cardiac pacing configurations were tested. Ultrasound measurements of the systole period were used as a reference and the improved method was compared with the original estimator. A reduction of 11% on the absolute estimation error was obtained for the systole period with the proposed algorithm switching approach.

Author Keywords Endocardial Acceleration ; Heart Sounds ; SonR ; Cardiac Resynchronization Therapy ; Algorithm Switching ; ECG

Introduction

Cardiac resynchronization therapy (CRT) is the therapy of choice for patients suffering from drug-refractory heart failure (HF) with significant inter- or intraventricular conduction delays [1]. A number of multicentric clinical trials have shown that CRT effectively improves cardiac function and, in general, the quality of life of most of these patients. However, approximately 30% of the implanted patients do not respond to the therapy [1]. One way to minimize the rate of non-responders would be to personalize the pacing parameters, particularly the atrioventricular (AV) and inter-ventricular (VV) activation delays, since these parameters have a significant impact on the cardiac function (ventricular contractility, cardiac output, transmitral flow, etc.) and their optimal configuration is patient-specific [2,3].

Currently, the optimization of these pacing parameters involves an echo-Doppler acquisition, to evaluate the ventricular mechanical function while scanning different values for AV and VV delays. Different echocardiographic markers have been analyzed in this context, such as the variations of cardiac output [3]. This is a complex and cumbersome method, which is not applied systematically and is typically performed at rest, in supine position, before the discharge of the patient from the hospital. An interesting alternative to this in-hospital, echocardiography-based approach would be to obtain a signal from an implantable sensor, capable of monitoring the mechanical cardiac function. This signal could be processed to extract a set of features, such as the systolic and diastolic time intervals, that could be used as control variables for an adaptive closed-loop AV and VV delay optimization. This approach would simplify and generalize the application of the AV and VV delay optimization stage, reducing costs, and would provide a better CRT delivery under different physiological conditions (rest, exercise, etc.).

Cardiac mechanoacoustic signals, such as the phonocardiogram (PCG) have been largely studied for the evaluation of the mechanical function of the heart, including the analysis of the effect of different CRT pacing configurations on systolic time intervals [4–7]. Recently, Sorin CRM SAS (Clamart, France) developed a piezo-electric micro-accelerometer inserted into the tip of an endocardial pacing lead (SonR sensor). This sensor provides an endocardial micro-acceleration signal, that may be useful for the continuous optimization of the delivered CRT [8–11]. This sensor could also provide complementary information that would be useful to improve remote patient follow-up and the early-detection of undesired events [12].

The SonR signal is composed of two main components, denoted here SonR1 and SonR2, that are synchronous with the first and second heart sounds in the PCG, respectively (see figure 1). We hypothesize that variations of the AV and VV pacing delays will induce modifications of the cardiac mechanical activity that can be monitored by a set of features extracted from the SonR signal.

In a previous work, we studied an external version of the SonR signal, and proposed a method to estimate the mitral and aortic valve closure instants [13]. This method was then clinically evaluated in the context of CRT optimization with data from 75 HF patients, under different pacing configurations [14]. We showed that satisfactory systolic/diastolic time interval estimations can be obtained from the SonR signal. For instance, a correlation coefficient of 0.85 with an average absolute estimation error of 13.4 ms was obtained for the estimation of the systole period. More details on the performance obtained for the different valve closing instants are provided in [14]. However, we also noticed that, according to the signal context (signal-to-noise ratio, instantaneous heart rate, etc…) of each record, the SonR signal processing methods providing the best performance were not the same. In the present paper, we propose an improvement of the original method, integrating an optimal combination of different detector configurations, in an algorithm switching approach.

Methods

Brief description of the original method and its parameters

The original detection method proposed in [14] analyzed the SonR signal and output the timing of SonR1 and SonR2. Briefly, after ensemble averaging and high-pass filtering, we applied signal envelope estimation and identified the onset of SonR1 and SonR2 by testing when the envelope exceeded specific thresholds. The following paragraphs provide some details on each of these processing phases and presents the notation that will be used throughout this paper.

As the first step, the instant of electrical activation of each beat (e.g. first pacing spike for pacing records or QRS detection in spontaneous rhythm) is performed on the available ECG to segment SonR signals into independent cardiac cycles. The ensemble averaging phase is performed separately on SonR1 and SonR2, from a group of 15 consecutive, correlated beats. This phase includes: i) the estimation of phase shifts that maximize the correlation between each observed cycle, ii) the alignment of each cycle with respect to the corresponding estimated phase-shift and iii) the calculation of the two average components SonR1 and SonR2. Only cycles with a normalized correlation coefficient greater than 0.6 for SonR1 and 0.5 for SonR2 were included in the averaging phase.

The obtained average cycles, $SonR(t)$, were then high-pass filtered with a cutoff frequency fc and the signal envelope was computed by applying method M and a moving average filter of size w. After normalization, a threshold λ was finally applied to detect the onset of SonR1 and SonR2, which will be respectively defined as τ^1 and τ^2.

Figure 1 presents an example of a processed average cycle, acquired from a CRT recipient during bi-ventricular pacing and showing the main detection instants, when using an envelogram computed with the absolute value method. Similar envelope estimation methods have been largely applied to the segmentation of PCG signals and it has been shown that their performance strongly depends on the tuning of fc, w, λ and M [4–7], [13].

Parameter optimization and performance evaluation

This section presents a method to optimize parameters fc, w, λ and M using data from a CRT patient population. The database used for learning and testing the optimal parameter set is firstly described. The parameter optimization method is then presented and, finally, a bootstrapping method is proposed to analyze the reproducibility of the optimal detector configuration as a function of the learning and test sets used.

Database

In this work we considered a subset of the database used in [14], containing 31 HF patients implanted with a biventricular system and enrolled by the Rennes University Hospital (CHU Rennes, Service de Cardiologie et Maladies Vasculaires). This database (*DB*) is composed of $N = 103$ records containing two standard ECG leads, surface SonR and pulsed Doppler echocardiography, acquired during various pacing configurations (biventricular pacing with various VV delays, single ventricular pacing, and spontaneous rhythm, when possible). For each pacing configuration, Doppler acquisitions were performed sequentially at the aortic and the mitral sites. An example of the acquired signals during the exploration of the aortic site is presented in figure 2.

A particular effort has been made to maximize the accuracy and reproducibility of the Doppler measurements. Doppler signals were processed by a custom-made software, in order to assist in the annotation of the valve closure instants. Semi-automatic annotations were thus performed for each record k ($k = 1, \ldots, N$) by a trained operator, validated by an independent echocardiographer over 3 to 6 selected cycles, and averaged. The systole interval obtained from the Doppler signals from record k, I_k^{sys}, calculated as the difference between the closure instant of the aortic valve and the closure instant of the mitral valve, will be used in this paper as the reference marker for performance evaluation. The estimation of the systole period implies a correct estimation of the closure instants of the mitral and aortic valves, and can be used to estimate the diastole period.

Optimization method

Rather than using an evolutionary algorithm, as we have proposed in previous works [15], parameter optimization was performed here by applying the above-mentioned detection method with all combinations of the following parameter values: $fc \in \{20, 25, 30\}$ Hz; $w \in \{60, 80, \ldots, 120\}$ ms and $M \in \{A, S\}$, where A and S represent, respectively, the absolute and squared envelope estimators. Thresholds were applied to individually normalized envelograms for SonR1 and SonR2 and were obtained from the set $\lambda \in \{0.1, 0.2, \ldots, 0.7\}$. The elements of these different parameter sets were defined within the ranges typically observed in the literature and from our previous experience in the processing of SonR and PCG signals [4–7,13].

The application of this pseudo-exhaustive research approach produced $N = 168$ different "detector configurations" D_i^{SonR1}, $i = 1, \ldots, N$ for the detection of the onset of SonR1 and D_j^{SonR2}, $j = 1, \ldots, N$ for the onset of SonR2. The couple $(D_i^{SonR1}, D_j^{SonR2})$ will be simply referred to as D, with $m = 1, \ldots, N_D^2$. It is worth noting that for some D, the detectors might fail to provide an estimation of $\hat{t}_{m,k}^{SonR1}$ and/or $\hat{t}_{m,k}^{SonR2}$. We have chosen to reject all D providing a rate of detection failure higher than 6%. For each D and each record k, an estimation $\hat{I}_{m,k}^{SYS}$ of the clinical reference measurement $I_{m,k}^{SYS}$ was obtained through a function f, such that

$$\hat{I}_{m,k}^{SYS} = f_L(\hat{t}_{m,k}^{SonR1}, \hat{t}_{m,k}^{SonR2}). \quad (1)$$

Function f was estimated by means of a multivariate linear regression during the learning phase and was kept fixed during the test phase. Detection performance was thus evaluated through the absolute estimation error:

$$\epsilon_{m,k}^S = \left|\hat{I}_{m,k}^{SYS} - I_{m,k}^{SYS}\right| \quad (2)$$

where $S = L$ when $\hat{I}_{m,k}^{SYS}$ is calculated with the learning dataset and $S = T$ when $\hat{I}_{m,k}^{SYS}$ is calculated with the test dataset (but with the fixed f function). Finally, the mean absolute error for configuration m is obtained by

$$\bar{\epsilon}_m^S = \frac{1}{N}\sum_{k=1}^{N} \epsilon_{m,k}^S, \quad (3)$$

where, again, S represents either the learning $S = L$ or the test $S = T$ datasets and N is the number of available records.

The optimal detector configuration D_{m^*} is thus selected as the configuration providing the lowest $\bar{\epsilon}_m^L$. However, as mentioned before, this optimal configuration depends strongly on the specific records included in the learning database. The next section proposes a bootstrapping method to quantify the influence of the learning and test datasets on the selection of D_{m^*} and the obtained detection performance.

Bootstrapping method

In order to evaluate the sensitivity of the optimal configuration to the learning and test sets, a bootstrapping method was used to create $N = 100$ different learning ($LDB(n) \subset DB$) and test ($TDB(n) \subset DB$, $n = 1, \ldots, N$) datasets. Each learning dataset is obtained by selecting randomly, without replacement, $N = 72$ records (70% of the available records in DB), while the corresponding test dataset was created with the resting $N = 31$ records.

The above-mentioned optimization procedure was applied to compute the absolute estimation error for each D, when applied to each record k of each realization n of the bootstrapping method. These errors are stored in $m \times k$ vectors $\epsilon_{m,k}^L(n)$ and $\epsilon_{m,k}^T(n)$ when using $LDB(n)$ and $TDB(n)$, respectively. Corresponding vectors containing the average absolute error over all records k, $\bar{\epsilon}_m^L(n)$ and $\bar{\epsilon}_m^T(n)$ were also calculated. The optimal detector configuration for a given realization of $LDB(n)$ is defined as $D_{m_n^*}^L$, where

$$m_n^* = \underset{m}{\operatorname{argmin}}(\bar{\epsilon}_m^L(n)). \quad (4)$$

Finally, we calculate the mean absolute error generated by each $D_{m_n^*}^L$ over all realizations of the bootstrapping method,

$$\mu_{\epsilon^L} = \frac{1}{N_B}\sum_{n=1}^{N_B} \epsilon_{m_n^*}^L(n) \quad (5)$$

and its standard deviation $\sigma_{\epsilon} L$. A similar approach has been applied to $TDB(n)$ to compute the average errors $\mu_{\epsilon} T$ and $\sigma_{\epsilon} T$, using configuration $D_{m_n^*}^L$.

A problem arises when we decide to implement these parameters in a real-life application: which of the parameter configuration should we use? We hypothesize that this dependence is partly related to the signal quality of each record and that detection performance can be improved by selecting the optimal set of parameters as a function of the signal context.

Algorithm switching method

The objective of the proposed algorithm switching approach is to select the detection configuration $D^L_{m^*_{n,q}}$ that optimizes a certain performance criterion and where the index q is obtained by quantization of a control variable c, which reflects the current signal context for $SonR(t)$. Similar approaches have been proposed in multimodel control systems, where quantization phase is based on a set of sharp or fuzzy rules [16]. In this paper, we present an approach that is adapted to a real-time implementation and is based on *a priori* knowledge on the response of each D to different signal contexts.

A diagram of the proposed detection approach is presented in figure 3. The algorithm is composed of the following phases:

SonR signal pre-processing

The raw SonR signal is processed to obtain the average cardiac cycle $SonR(t)$, as presented in section II.A.

Signal context estimation

A control variable $c \in \mathbb{R}$, representing the current signal context, is estimated for each pre-processed signal $SonR(t)$. Different features extracted from $SonR(t)$ were considered for the control variable c: i) the instantaneous heart rate, ii) the interbeat SonR1 and SonR2 correlation coefficients, iii) SonR1 and SonR2 peak to peak amplitudes and iv) the SonR1 contrast, defined as the ratio between the peak to peak amplitude of SonR1 and the standard deviation of the first 300 milliseconds of signal $SonR(t)$.

Quantile selection

Variable c is quantized by means of a classical quantile selection approach to obtain the switch variable $q \in \{1, \ldots, Q\}$. The Q-quantiles of the distribution of each c are estimated using the entire database DB, and subsets $C = \{k \mid c \text{ quantile}\}$ are constructed.

Context-dependent optimal detector configurations

The objective of the proposed algorithm switching approach is to select an optimal configuration $D^L_{m^*_{n,q}}$, according to the quantile membership q of the current signal context c. This configuration will be applied to the signal processing chain, including high-pass filtering, envelope estimation, thresholding and multilinear modeling, to finally obtain an estimation of the systolic period $\hat{I}^{sys}_{m,k}$.

In order to identify these optimal configurations, the bootstrapping method described in the previous section was applied. However, in this case, equation 4 is adapted to provide the optimal configuration as a function of q,

$$m^*_{n,q} = \underset{m}{\operatorname{argmin}} \left(\sum_{k \in C_q} \frac{\epsilon^L_{m,k}(r_n)}{|C_q|} \right)$$

(6)

where $|C$ is the cardinality of C. The absolute error obtained when using the algorithm switching approach for record k and a given realization of $LDB(n)$ will be noted $\epsilon^L_{m^*_{n,q},k}(r_n)$. The average absolute error is thus defined in this case by

$$\epsilon^L_{as}(r_n) = \frac{1}{N_L} \sum_{q=1}^{Q} \sum_{k \in C_q} \epsilon^L_{m^*_{n,q},k}(r_n).$$

(7)

We finally calculate the global indicators:

$$\mu^{as}_{\epsilon^L} = \frac{1}{N_B} \sum_{n=1}^{N_B} \epsilon^L_{as}(r_n)$$

(8)

and its standard deviation $\sigma^{as}_{\epsilon^L}$. Configurations $D^L_{m^*_{n,q}}$ are then tested on each $TDB(n)$ to obtain the reference testing indicators $\mu^{as}_{\epsilon^T}$ and $\sigma^{as}_{\epsilon^T}$.

Results and Discussion

Optimal configurations of the original detection method

Table I presents the optimal configurations of the original detection method $D_{m^*_n}$, for a random selection of 10 realizations of the bootstrapping approach. It is worth noting that the optimal detector parameters vary from one realization to the other, meaning that the

optimal detector configuration depends on the selection of records constituting the learning database. This is particularly true for the detection of SonR1. For example, the range of optimal values for parameter *w* varies from 80 ms (leading to a sharp envelope) to 140 ms (generating a very smooth envelope).

The mean absolute error generated by each $D^L_{m_n^*}$ over the 100 realizations of the learning database (*LDB*(*n*)) equals $\mu_\varepsilon L = 12.4ms$ with a standard deviation $\sigma_\varepsilon L = 0.6$ *ms*. The application of the optimal configurations $D^L_{m_n^*}$ on the corresponding realization of the test dataset *TDB*(*n*) yielded a higher mean absolute error, $\mu_\varepsilon T = 14.5$ *ms* and standard deviation $\sigma_\varepsilon T = 1.7$ *ms*, as expected.

A Bland-Altman plot comparing $\hat{I}^{SYS}_{m,k}$ versus $I^{SYS}_{m,k}$, for a representative realization of *TDB*(*n*) (*n* = 41) is presented in figure 4. The mean absolute error for this realization was $\varepsilon^T_{m_n^*} = 14.61ms$, which is close to $\mu_\varepsilon T$. No particular distribution can be observed on the plot, and only one estimation was out of the limits of agreement for this realization. These results are in line with those obtained in our previous works with the same patient population and will be used as reference to evaluate the impact of the proposed algorithm switching method on detection performance.

Algorithm switching method

Tests have been performed with *Q* = 2, *Q* = 4 and *Q* = 8. Results will only be shown for 4 quantiles, since this was the best tradeoff between algorithm complexity and detection performance.

Results obtained from the application of the algorithm switching method, for three different control variables (SonR1 contrast, as defined in section II.C, instantaneous heart rate and the amplitude of the SonR2 component) and the 100 realizations of the bootstrapping method are summarized in Table II. For all the tested control variables, the mean absolute estimation error was reduced with respect to the reference values. For instance, with control variable "SonR1 contrast", the learning error is $\mu^{as}_{\epsilon^L} = 10.8ms$ whereas it was $\mu_\varepsilon T = 12.4$ *ms* without algorithm switching: the observed learning gain is 1.6 *ms* or 13%. Concerning the testing results, the error decreases from $\mu_\varepsilon T = 14.5$ *ms* to $\mu^{as}_{\epsilon^T} = 12.8ms$: the testing gain is 11%. In all cases, the gain was statistically significant

($p < 0.001$ observed with a bilateral paired t-test). Although the values of $\sigma^{as}_{\epsilon^L}$ and $\sigma^{as}_{\epsilon^T}$ are globally similar to the reference values, they are lower than the reference when using SonR1 contrast or SonR2 amplitude as control variables. This result shows that the proposed approach allows for a more robust estimation of $I^{SYS}_{m,k}$ than the original method, being thus less sensitive to overfitting. We can also mention that, in all cases, there was no increase in the miss-detection rate, which was still under the 6% limit.

Figure 5 shows a Bland-Altman plot obtained with the algorithm switching method using the SonR1 contrast variable. Realization *n* = 41 of *T DB*(*n*) was also used in this figure. A mean absolute error of $\varepsilon^T_{m_n^*} = 12.63ms$ was observed for this realization. The Bland-Altman plot properties for the algorithm switching approach are similar to those of the original detector (Figure 4), but present a lower dispersion. Indeed, the effect of the proposed method can be observed when comparing individual points on both plots. Records presenting the highest and lowest performance gain when applying the proposed approach are marked respectively with a star (*) and a triangle (Δ) in figures 4 and 5. The highest gain was of 23.3 *ms* and the lowest was of −6.6 *ms*.

Conclusion

Previous studies have shown that the use of cardiac mechanoacoustic signals may be useful for the assessment of the mechanical function of the heart. A number of signal processing methods have been proposed to estimate the most significant events of the cardiac cycle from these signals. However, the optimal configuration of these detectors remains a challenging problem. In this paper, we have proposed a generic algorithm switching method that activates an optimal configuration for the applied signal processing chain, as a function of the current signal context.

The proposed method has been quantitatively evaluated using data from a population of 31 patients suffering from chronic heart failure and implanted with a biventricular pacemaker, so as to estimate the systolic period for different pacing configurations, through the analysis of a cardiac micro-acceleration signal (SonR). A bootstrapping method was applied to i) estimate the sensitivity of the optimal detector configuration to a given couple of learning and test datasets and ii) evaluate the benefits of using the proposed algorithm switching approach. Results show that modifications of the signal-to-noise ratio, but also of the instantaneous heart rate, on the records constituting the learning dataset have an impact on the definition of the optimal detector configuration. In this context, the application of the proposed algorithm switching method provides a statistically significant performance improvement with respect to the original detector of more than 11% in the estimation of the systole period (and hence, diastole period) from the SonR signal. Although interesting, this improvement may however be of limited impact on some clinical applications, in which variations of less than 3 *ms* on the systolic and diastolic periods can be neglected.

Additional developments may improve even further the obtained results. Indeed, although the semi-automatic approach for Doppler annotation showed significantly higher interoperator reproducibility than the manual method, the interoperator estimation error for the

systole interval reached 7 *ms* on a set of 10 patients randomly selected from *DB* [14]. The proposed method provides thus an absolute error that approaches the variability of the reference. A new clinical protocol is being designed to acquire the SonR signal synchronously with invasive blood pressure signals during the implant of the pacemaker. These data will provide a better reference than the Doppler method. Furthermore, although results from the bootstrapping method provided encouraging information about the improved robustness and generalization capabilities of the proposed method with respect to the original approach, an evaluation on a database with a higher number of patients should be performed.

Finally, results also show that the estimator's performance depends on other aspects than the signal context. An additional improvement may thus be found by optimizing detector configurations in a patient-specific manner. Current works are directed towards the estimation of these patient-specific configurations and also to the extension of the proposed method to multiple, concurrent control variables and a fuzzy quantile selection function.

Acknowledgements:

This work was supported in part by the French National Agency of Research under grant ANR-08-TECS013.

References:

- 1 . Dickstein K , Vardas P , Auricchio A , Daubert J , Linde C , McMurray J , Ponikowski P , Priori S , Sutton R , van Veldhuisen D . 2010 focused update of esc guidelines on device therapy in heart failure . Europace . 12 : (11) 1526 - 2010 ;
- 2 . Auricchio A , Stellbrink C , Block M , Sack S , Vogt J , Bakker P , Klein H , Kramer A , Ding J , Salo R . Effect of pacing chamber and atrioventricular delay on acute systolic function of paced patients with congestive heart failure . Circulation . 99 : (23) 2993 - 3001 1999 ;
- 3 . Sun JP , Lee APW , Grimm RA , Hung MJ , Yang XS , Delurgio D , Leon AR , Merlino JD , Yu CM . Optimisation of atrioventricular delay during exercise improves cardiac output in patients stabilised with cardiac resynchronisation therapy . Heart . 98 : (1) 54 - 59 Jan 2012 ;
- 4 . Durand LG , Pibarot P . Digital signal processing of the phonocardiogram: review of the most recent advancements . Crit Rev Biomed Eng . 23 : (3–4) 163 - 219 1995 ;
- 5 . Liang H , Lukkarinen S , Hartimo I . Heart sound segmentation algorithm based on heart sound envelogram . Proc. Computers in Cardiology 7–10 Sept. 1997 105 - 108
- 6 . Gill D , Gavrieli N , Intrator N . Detection and identification of heart sounds using homomorphic envelogram and self-organizing probabilistic model . Proc. Computers in Cardiology Sept. 25–28, 2005 957 - 960
- 7 . Marcus FI , Sorrell V , Zanetti J , Bosnos M , Baweja G , Perlick D , Ott P , Indik J , He DS , Gear K . Accelerometer-derived time intervals during various pacing modes in patients with biventricular pacemakers: comparison with normals . Pacing Clin Electrophysiol . 30 : (12) 1476 - 1481 Dec 2007 ;
- 8 . Plicchi G , Marcelli E , Parlapiano M , Bombardini T . Pea i and pea ii based implantable haemodynamic monitor: pre clinical studies in sheep . Europace . 4 : (1) 49 - 54 Jan 2002 ;
- 9 . Dupuis JM , Kobeissi A , Vitali L , Gaggini G , Merheb M , Rouleau F , Leftheriotis G , Ritter P , Victor J . Programming optimal atrioventricular delay in dual chamber pacing using peak endocardial acceleration: comparison with a standard echocardiographic procedure . Pacing Clin Electrophysiol . 26 : (1 Pt 2) 210 - 213 Jan 2003 ;
- 10 . Bordachar P , Labrousse L , Ploux S , Thambo JB , Lafitte S , Reant P , Jais P , Haissaguerre M , Clementy J , Santos PD . Validation of a new noninvasive device for the monitoring of peak endocardial acceleration in pigs: implications for optimization of pacing site and configuration . J Cardiovasc Electrophysiol . 19 : (7) 725 - 729 Jul 2008 ;
- 11 . Delnoy PP , Marcelli E , Oudeluttikhuis H , Nicastia D , Renesto F , Cercenelli L , Plicchi G . Validation of a peak endocardial acceleration-based algorithm to optimize cardiac resynchronization: early clinical results . Europace . 10 : (7) 801 - 808 Jul 2008 ;
- 12 . Le Rolle V , Ojeda D , Hernández A . Embedding a cardiac pulsatile model into an integrated model of the cardiovascular regulation for heart failure followup . Biomedical Engineering, IEEE Transactions on . 58 : (10) 2982 - 2986 oct 2011 ;
- 13 . Giorgis L , Hernández A , Amblard A , Senhadji L , Cazeau S , Jauvert G , Donal E . Analysis of cardiac micro-acceleration signals for the estimation of systolic and diastolic time intervals in cardiac resynchronization therapy . Proc Computers in Cardiology . 2008 ; 393 - 396
- 14 . Donal E , Giorgis L , Cazeau S , Leclercq C , Senhadji L , Amblard A , Jauvert G , Burban M , Hernández A , Mabo P . Endocardial acceleration (sonr) vs. ultrasound-derived time intervals in recipients of cardiac resynchronization therapy systems . Europace . 13 : (3) 402 - 408 Mar 2011 ;
- 15 . Dumont J , Hernández A , Carrault G . Improving ecg beats delineation with an evolutionary optimization process . Biomedical Engineering, IEEE Transactions on . 57 : (3) 607 - 615 2010 ;
- 16 . Pags O , Caron B , Ordnez R , Mouille P . Control system design by using a multi-controller approach with a real-time experimentation for a robot wrist . International Journal of Control . 75 : 1321 - 1334 2002 ;

Fig. 1

Surface electrocardiogram (ECG) and mechanoacoustic (SonR) signals obtained from a CRT recipient during bi-ventricular pacing. (a) average surface ECG computed from 15 consecutive cycles, (b) average SonR cycle computed from 15 consecutive cycles, displayed with the detected onset instants for SonR1 and SonR2, (c) high-pass filtered SonR cycle in (b) with its envelope. Time t=0 corresponds to the first ventricular event (right ventricular pacing spike in this case).

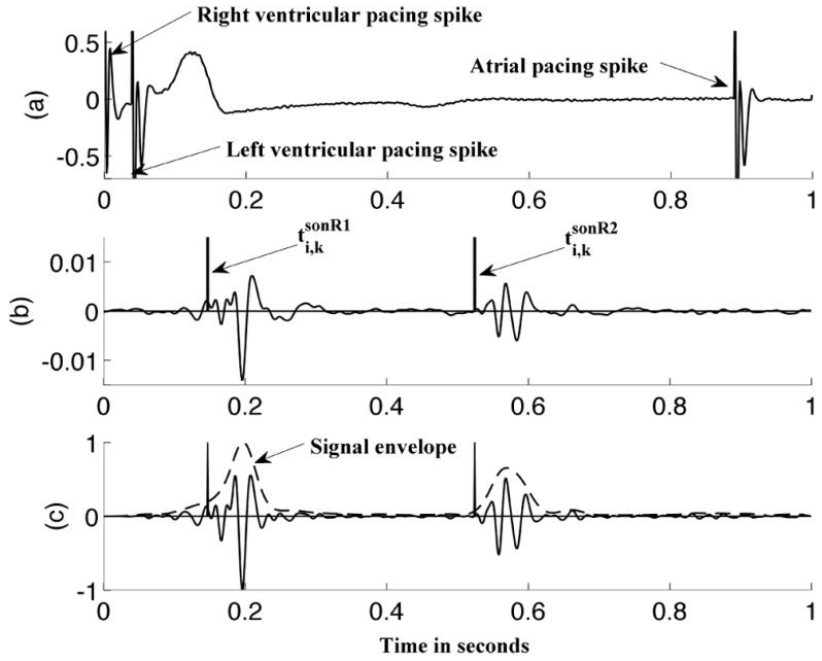

Fig. 2

Synchronous ECG (top panel), raw surface SonR (middle panel) and pulsed Doppler signal at the aortic site (lower panel), showing three beats from a record of the database. Pacing spikes were detected from the ECG signal and projected as segmented lines on the SonR signal. Segmented white lines on the Doppler signal represent the annotated opening and closure instants of the aortic valve for each beat.

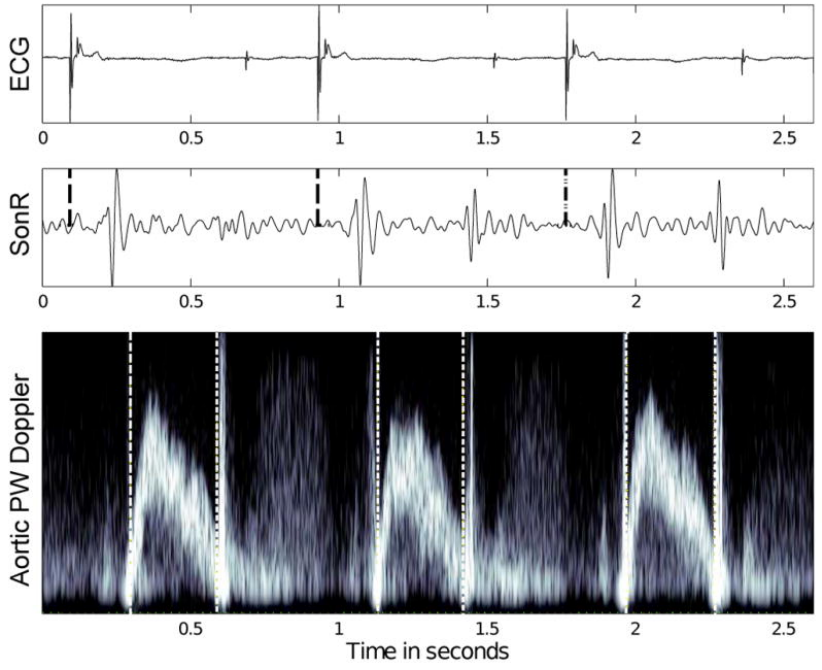

Fig. 3

General diagram of the proposed algorithm switching detector.

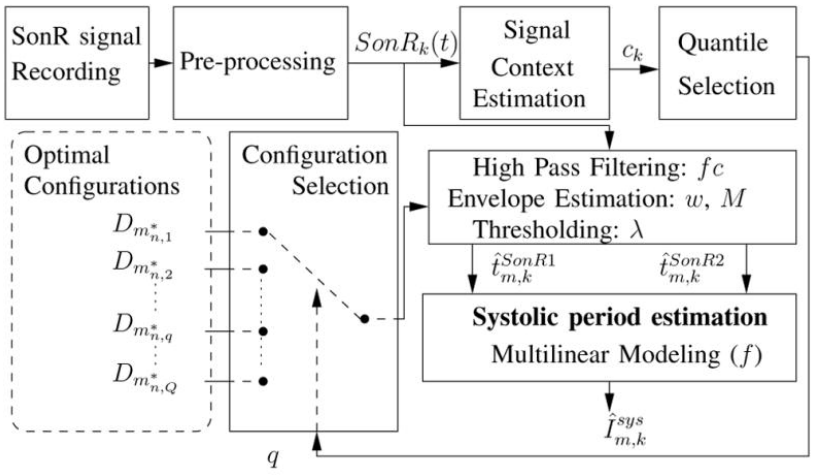

Fig. 4

Bland-Altman plot comparing the reference systole period, estimated from the echo Doppler signal (I_k^{sys}), with the estimated systole period ($\hat{I}_{m,k}^{sys}$) using the original detector and data from a representative realization (*n* = 41) of the testing dataset *TDB*(*n*).

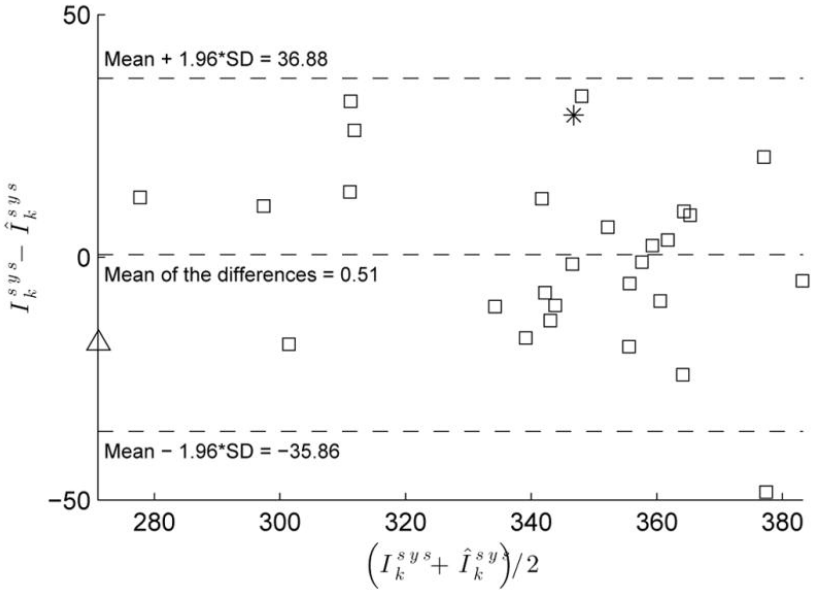

Fig. 5

Bland-Altman plot comparing the reference systole period, estimated from the echo Doppler signal (I_k^{sys}), with the estimated systole period ($\hat{I}_{m,k}^{sys}$) obtained with the proposed algorithm switching method using the SonR1 contrast variable. Data from realization n = 41 of the testing dataset $T\,DB(n)$ was used. Points * and Δ represent, respectively, the records with the highest and lowest performance gain with respect to the original method.

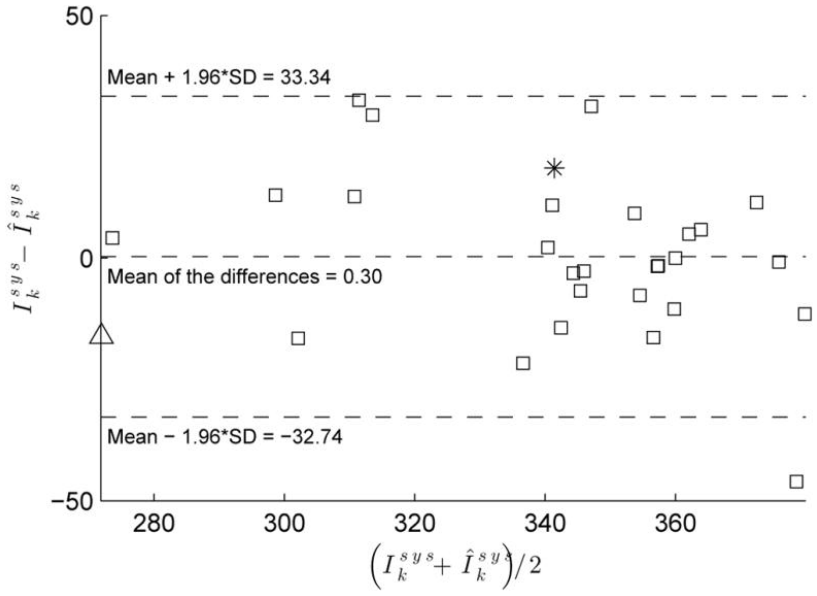

TABLE I

Random selection of 10 optimal detector configurations for the detection of SonR1 ($D_{i^*}^{SonR1}$) and SonR2 ($D_{j^*}^{SonR2}$), taken from the 100 realizations of the bootstrapping method. The parameters included in each detector configuration are: *M* -Envelogram type (A-absolute and S-squared envelograms), *w*-Smoothing window duration, λ-Threshold coefficient and *fc*-High-pass filter cutoff frequency. The mean absolute detection error is presented for each configuration.

	Optimal detector configuration for SonR1 ($D_{i^*}^{SonR1}$)				**Optimal detector configuration for SonR2 ($D_{j^*}^{SonR2}$)**				**Mean absolute detection error for the learning (L) and test (T) sets**	
Bootstrapping realization *n*	***M***	***w* (ms)**	λ	***fc*(*Hz*)**	***M***	***w* (ms)**	λ	***fc* (Hz)**	$\bar{\varepsilon}_{mn^*}^{L}(n)$ **(ms)**	$\bar{\varepsilon}_{mn^*}^{T}(n)$ **(ms)**
4	*A*	100	0.3	20	*S*	60	0.2	30	12.6	13.3
14	*A*	100	0.3	20	*S*	60	0.2	30	11.7	15.0
42	*S*	80	0.1	20	*S*	60	0.2	30	12.9	12.7
49	*A*	100	0.3	20	*S*	60	0.2	30	10.7	19.0
66	*A*	140	0.3	30	*S*	60	0.2	30	13.1	12.3
79	*A*	120	0.2	30	*S*	60	0.2	30	13.3	11.7
80	*S*	80	0.1	20	*S*	60	0.2	30	12.0	14.6
92	*A*	60	0.2	30	*A*	140	0.5	30	11.8	16.1
96	*A*	120	0.2	30	*A*	60	0.5	30	13.1	11.7
99	*A*	80	0.2	30	*A*	120	0.6	30	11.7	15.8

TABLE II

Best algorithm switching control variables and their associated average performance.

$\mu_{\epsilon^S}^{as}(ms)$

and

$\sigma_{\epsilon^S}^{as}(ms)$

represent respectively the mean absolute error and standard deviation, calculated over the 100 realizations of the bootstrapping method during the learning phase ($S = L$) or the test phase ($S = T$). Results obtained from the original method are shown as reference.

Control Variable (*c*)	$\mu_{\epsilon}^{\mathbf{Las}}$	$\sigma_{\epsilon}^{\mathbf{Las}}$	$\mu_{\epsilon}^{\mathbf{Tas}}$	$\sigma_{\epsilon}^{\mathbf{Tas}}$
SonR1 contrast	10.8	0.6	12.9	1.5
Heart Rate	11.1	0.6	13.9	1.8
SonR2 amplitude	11.2	0.6	13.6	1.6
	$\mu_{\epsilon}\boldsymbol{L}$	$\sigma_{\epsilon}\boldsymbol{L}$	$\mu_{\epsilon}\boldsymbol{T}$	$\sigma_{\epsilon}\boldsymbol{T}$
Reference results	12.4	0.6	14.5	1.7